Journal of Alloys and Compounds 509 (2011) 8239–8245

Contents lists available at ScienceDirect

Journal of Alloys and Compounds

journal homepage: www.elsevier.com/locate/jallcom

The microstructural characteristics and mechanical properties of Ni–Al/h-BN coatings deposited using plasma spraying

W.T. Hsiao[a,d,1], C.Y. Su[a,*], T.S. Huang[b,2], W.H. Liao[c,d,3]

[a] Graduate Institute of Manufacturing Technology, National Taipei University of Technology, Taipei 106, Taiwan
[b] China Steel Corporation, Kaohsiung, Taiwan
[c] Nano Technology Laboratory, Department of Materials Engineering, National Chung Hsing University, Taichung 402, Taiwan
[d] Materials and Chemical Research Laboratories, Industrial Technology Research Institute, Chutung 310, Taiwan

ARTICLE INFO

Article history:
Received 16 April 2011
Received in revised form 22 May 2011
Accepted 24 May 2011
Available online 6 June 2011

Keywords:
Plasma spraying
Coatings
Hexagonal boron nitride
Nickel aluminum

ABSTRACT

Hexagonal boron nitride (h-BN) material was added to a nickel aluminum alloy (Ni–Al), which was deposited as plasma spray coatings, and the resultant enhanced tribological properties of these coatings were investigated. The microstructures of the coatings were analyzed using a scanning electron microscope (SEM) to monitor the morphologies of both the powders and the coatings. After wear testing, the surface morphologies of the scratched coatings were analyzed using an SEM to monitor the fracture mode of the coatings. The results of this study indicate that the addition of h-BN material to Ni–Al results in coatings with enhanced tribological properties.

1. Introduction

The protection of machine part substrates is seriously considered by engineers and scientists. Substrate protection issues include wear, corrosion and oxidation resistance, and these issues arise when mechanical parts are operated under various environmental conditions. Fortunately, there are many ways to resolve these issues. For example, the deposition of protective coatings on the surfaces of mechanical parts is one way to improve their surface properties. These coatings are designed to enhance substrate surface properties, including tribology, corrosion resistance and oxidation resistance, at either normal or high temperatures [1,2]. Thermal spraying is a deposition method that can be used to apply suitable coatings onto machine parts so as to reduce wear loss [3,4]. Previous studies have shown that the thermal spraying of coatings provides good protection in terms of tribology or corrosion resistance, and this process has been ubiquitously used in industrial applications [5,6]. Plasma spraying is a high-energy variation of the thermal spraying deposition process and uses a high-temperature plasma torch to melt the powder materials. During the plasma spray process, feedstock powder is injected into a high temperature plasma torch, and the high melting energy used in the plasma spray process can be used to deposit dense coatings [7].

Protective coatings are necessary to provide high-temperature oxidation and corrosion resistance to machine parts to extend their life expectancy even in harsh environments and especially at high temperatures. The nickel aluminum (Ni–Al) alloy is a common high-temperature protective coating that can be easily deposited using thermal spraying. This alloy possesses good mechanical properties, oxidation resistance and corrosion resistance at high temperatures (>800 °C) [8,9]. The application of a lubricating material to Ni–Al coatings is one way to enhance the tribological properties of these coatings, which could prolong the life expectancy of machine parts.

Hexagonal boron nitride (h-BN) is a useful reinforcing material and has a low density, excellent stability and high thermal conductivity. It is also a good lubrication material due to its low coefficient of friction [10,11]; however, pure h-BN is difficult to deposit as a thermally sprayed coating due to its high melting temperature and weak bond strength at basal plane. Previous research has shown that h-BN can be trapped in a metallic matrix [12], which may represent one method of trapping h-BN material in a powder for use as a composite material in plasma spraying. Moreover,

* Corresponding author at: 1, Sec. 3, Chung-hsiao E. Rd., Taipei, 10608, Taiwan. Tel.: +886 2 27716117.
E-mail addresses: Jesse_Hsiao@itri.org.tw (W.T. Hsiao), cysu@ntut.edu.tw (C.Y. Su), 152827@mail.csc.com.tw (T.S. Huang), xhan@itri.org.tw (W.H. Liao).
[1] Address: Bldg. 79, 195, Sec. 4, Chung Hsing Rd., Chutung, Hsinchu 310, Taiwan. Tel.: +886 3 5915218; fax: +886 3 5820063.
[2] Address: 1 Chung Kang Road, Hsiao Kang, Kaohsiung, Taiwan. Tel.: +886 7 8051111x2999; fax: +886 7 8051107.
[3] Address: Bldg. 79, 195, Sec. 4, Chung Hsing Rd., Chutung, Hsinchu 310, Taiwan. Tel.: +886 3 5914101; fax: +886 3 5820063.

0925-8388/$ – see front matter © 2011 Elsevier B.V. All rights reserved.
doi:10.1016/j.jallcom.2011.05.095

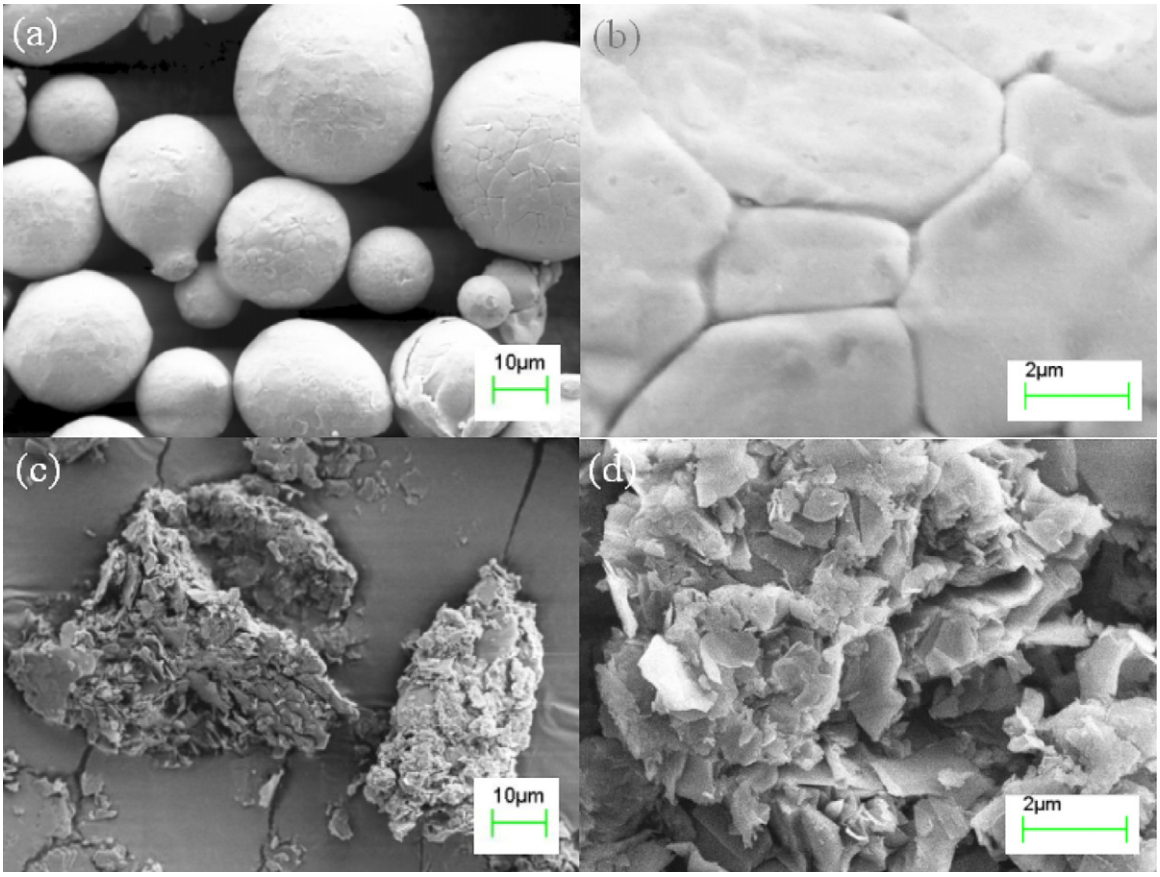

Fig. 1. SEM images of powders: (a) and (b) C1 powder, (c) and (d) h-BN powder.

mechanical alloying (MA) processes can be used to trap h-BN material as a composite powder for thermal spray deposition [13,14]. In previous studies, the addition of h-BN material as a solid lubricant in thermal spray coatings has been used to enhance the tribology properties of these coatings [15]. In this study, h-BN was added to thermal spray coatings to improve the tribological properties of these coatings at high temperature. Both MA and blended processes were used to prepare Ni–Al/h-BN powders before they were plasma sprayed as coatings.

2. Materials and methods

Ni–5 wt% Al powder with particle size 16–45 μm, which was produced by the PAC company, USA, was used in this study. Hexagonal boron nitride powder that contained 99.2% pure h-BN was produced by the Kallex Company Ltd., Taiwan. Thermal spraying was used to deposit approximately 200-μm-thick coatings on 25 mm × 25 mm × 5 mm 304 stainless steel substrates for the fabrication of metallographic and wear-testing specimens. The deposited materials are summarized in Table 1. Ni–5Al (Ni–5 wt% Al) and Ni–10BN–2.5Al (Ni–5 wt% Al + 10 wt% h-BN) powders were deposited using plasma spraying. Two types of Ni–10BN–2.5Al composite powders were used in these experiments. One composite powder was prepared using the blend method, whereas the other was prepared using ball milling as a mechanically alloying process. These composite powders were fed into a plasma spraying torch and deposited as coatings. The plasma-spray-deposited coatings of the Ni–5Al, Ni–10BN–2.5Al blend composite and the Ni–10BN–2.5Al MA composite material are designated as C1, C2 and C3, respectively in this study. Ball milling was performed using a Fritsch Pulverisette 5 planetary ball mill with a sufficient amount of the aforementioned powders prior to plasma spraying. For each vial of the ball mill, 100 g of composite powder was mixed using hardened stainless steel balls that were 7.92 mm in diameter and sealed in a stainless steel vial. The total weight of the balls was 594 g, and the milling time for each mixture was 4 h (each was mixed for 15 min and allowed to stand for 15 min) at 250 rpm.

Plasma spraying was used to deposit the coatings. An F4 plasma spraying gun (Sulzer Metco), using 55 SLPM argon and 9.5 SLPM hydrogen as the plasma gases, was used to produce the thermal spray coatings. The spraying parameters are shown in Table 2. The abrasion properties of the resultant coatings were characterized by dry sand wear testing based on the ASTM G65 standard. The wear load and wear distance during dry sand wear testing were 5 N and 60 m, respectively. The tribological properties of the coatings were tested using a ball-on-disk wear-testing instrument (UMT-2 MultiSpecimen Test System, CETR, USA). This instrument is equipped with heating coils to reach and maintain at a desired temperature. 440-C stainless steel balls with a diameter of 4.0 mm and HRC 62 microhardnesses at a load of 5 N were used for the wear testing. The wear distance and testing temperature were 20 m and 850 °C, respectively. After wear testing, the morphologies of the worn surfaces were analyzed using a scanning electron microscope (SEM). Bond testing of the coatings was performed according to the ASTM C 633 standard. The bond strengths of the coatings were averaged over eight positional points.

X-ray diffraction (XRD), metallurgical microscopy, scanning electron microscopy and energy dispersive spectrometry (EDS) were used to analyze the microstructures of the thermal spray coatings. An epoxy resin that had been treated with glass sand, which helps increase the hardness of the resin, was used for the sample preparation. All samples were ground and polished before observation. The porosity of the coatings was analyzed using Image Pro Plus (Media Cybernetics, Inc.).

Table 1
Materials in the thermal spray coatings.

Samples	Coating material	Mixed method
C1	Ni–5Al	
C2	Ni–10BN–2.5Al	Blend
C3	Ni–10BN–2.5Al	MA

Table 2
Plasma spraying parameters.

Argon	Hydrogen	Current	Carrier gas	Spray distance	Robot speed
55 SLPM	9.5 SLPM	600 A	3.5 SLPM	140 mm	400 mm/s

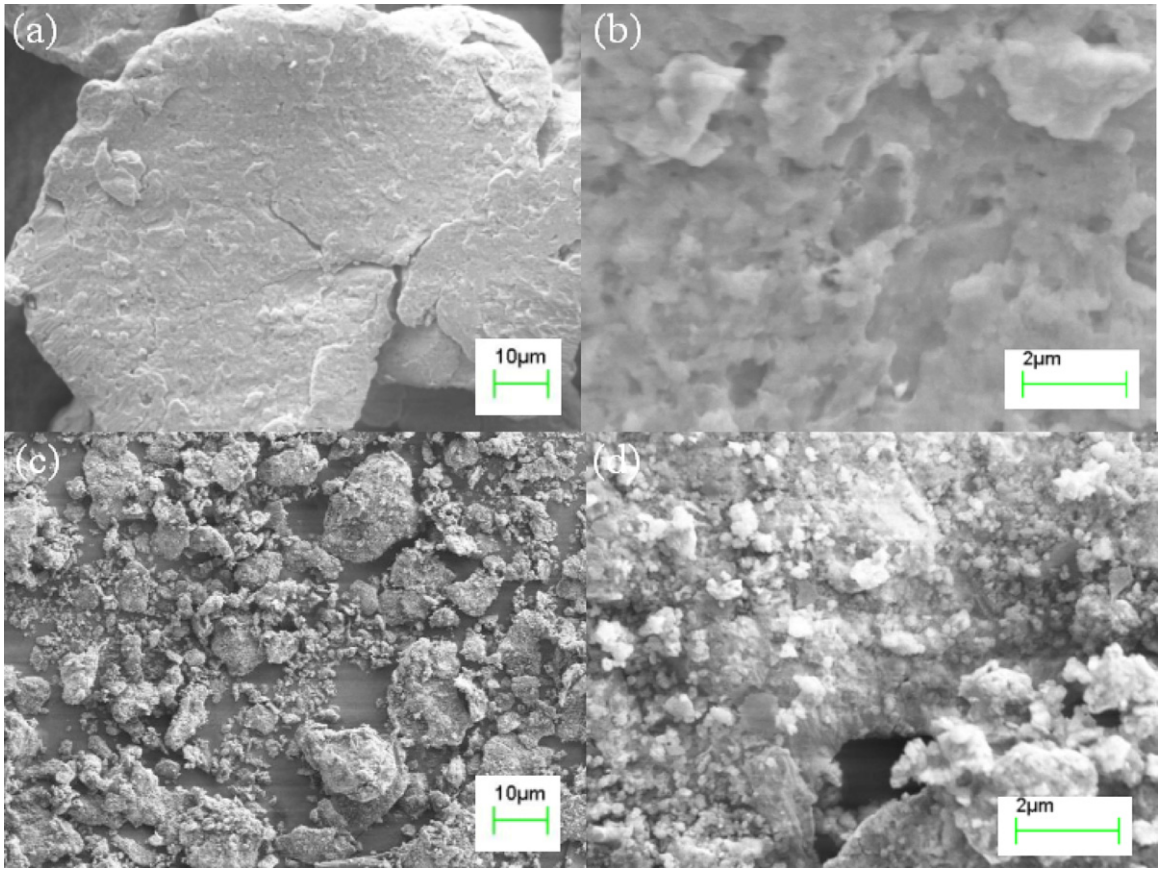

Fig. 2. SEM images of MA powders: (a) and (b) C1 powder after 4 h of MA, (c) and (d) C3 powder after 4 h of MA.

3. Results and discussion

Figs. 1 and 2 depict the SEM images of the powders that were used as the feed material in this study. The particle morphology of the C1 powder was spherical and crystalline, as shown in Fig. 1(a) and (b); the particle size distribution of the Ni–Al alloy powder was 16–45 μm. After the C1 powder was prepared using MA, the morphology of each C1 MA particle became flaky. Moreover, the dimensions of the particles were broader and thinner than those of the particles before the MA process, and no broken Ni–Al particles were observed following the MA process (Fig. 2(a) and (b)). The morphology of the h-BN material exhibited a flaky microstructure, as shown in Fig. 1(c); however, weak adhesion between the flakes was observed, as shown in Fig. 1(d). To prepare the composite powder, h-BN powder was added to the C1 powder using the blend and MA techniques, and then the powders were deposited as coatings C2 and C3. The particle size of the C3 composite powder (Fig. 2(c) and (d)) was smaller than that of the C1 and h-BN powders. The h-BN material separated the Ni–Al particles from each other, which resulted in a decreased particle size after the MA process. The h-BN powder was dispersed and distributed around the Ni–Al particles due to the MA process.

The C1, C2 and C3 coatings were prepared using spherical Ni–Al powder, blended powder and MA powder, respectively. The deposition rates of the C1 coating was higher than those of the other aforementioned composite coatings. When h-BN was added to the coating, the coating deposition rate decreased, as shown in Fig. 3. Moreover, the deposition rate of the C3 coating was slower than that of the C2 coating. As shown in Fig. 2(c), smaller particles were obtained after the MA process, resulting in a slower C3 coating deposition rate.

An SEM image of the cross-sectional microstructure of the C1 coating exhibits a high density (Fig. 4(a)), and the microstructure depicted in this figure has a low porosity. Significant splat boundaries that are located between the lamellar structures of the coating can be observed in the high-magnification image depicted in Fig. 4(b). EDS analysis identified higher Al and O elemental contents in the gray area that are designated by the arrow in the figure. Similar Al- and O-rich areas were observed in the C2 and C3 coatings. Similar structures with oxide phases have also been observed in others studies [16,17]. Fig. 4(c) and (d) depicts microstructural images of the C2 coating and, as the figure indicates, the addition

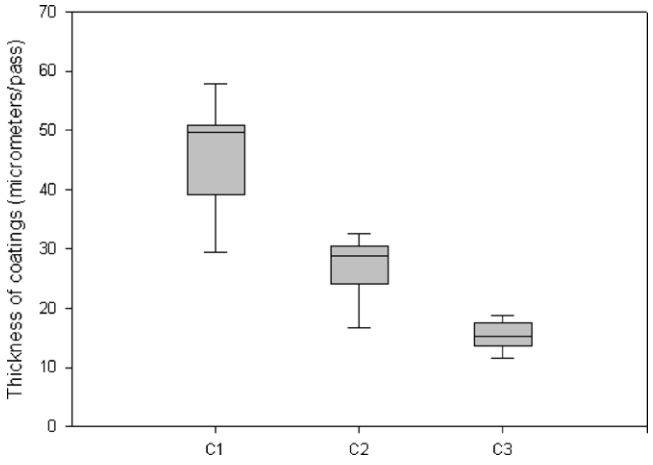

Fig. 3. Deposition rates of the various coatings.

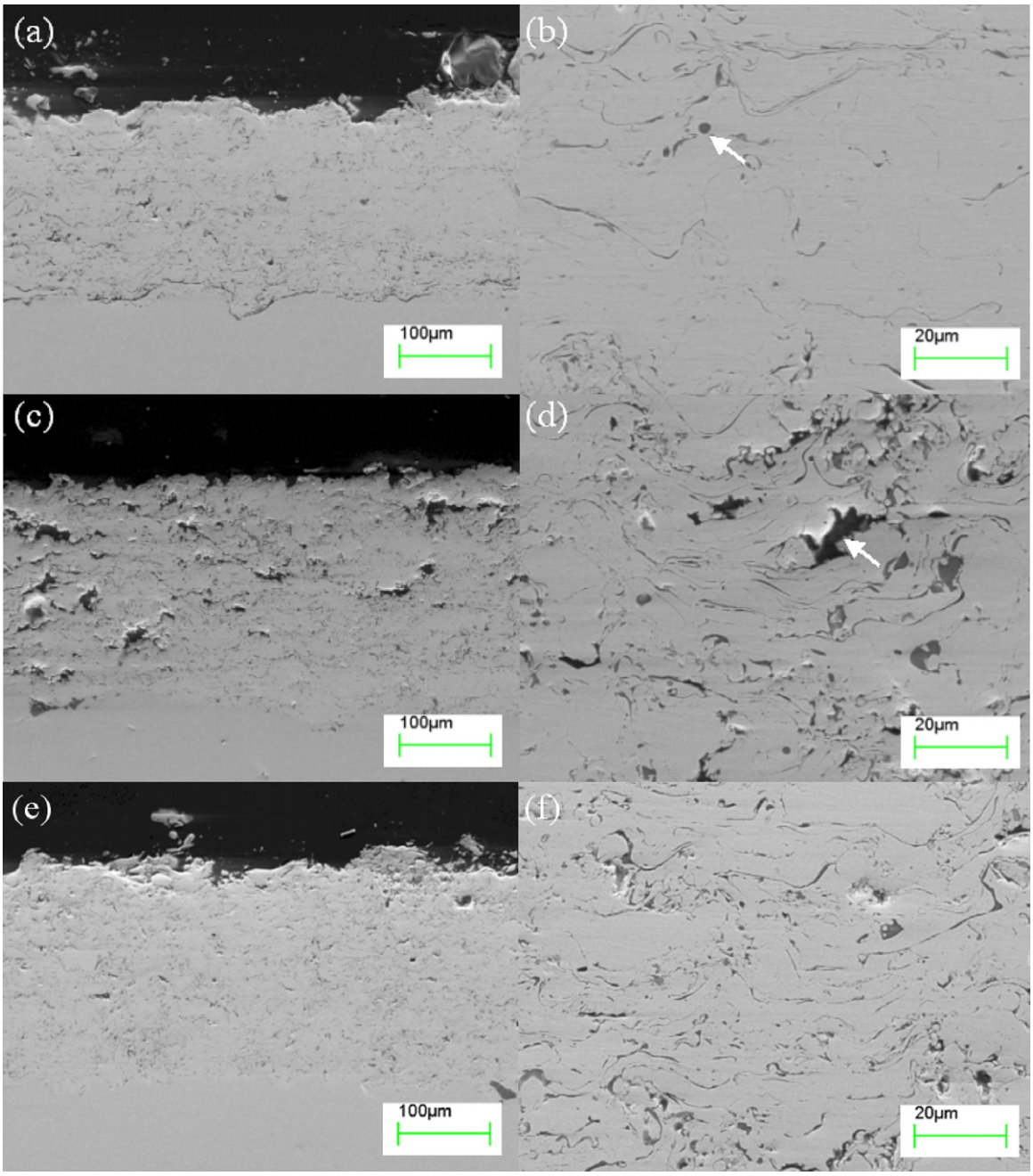

Fig. 4. SEM images of coatings created using atmosphere plasma spraying: (a) and (b) C1 coating, (c) and (d) C2 composite coating and (e) and (f) C3 composite coating.

of h-BN to the C2 coating increased the coating's porosity compared to that of the C1 coating. In addition, the interface between the lamellar structures was significant in the C2 coating. Higher B and N contents were observed at the splat boundaries and porous areas, as indicated by the arrow shown in Fig. 4(d) and as determined using EDS analysis. Based on a comparison of the C1 and C2 coatings, the BN that is located in the splat boundary position could explain the increase in porosity because it is a lubricating material; however, because h-BN was added to the Ni–Al powder and processed via MA, the C3 powder was refined. Therefore, after plasma spraying, the porosity of the C3 coating exhibited a lower porosity than that of the C2 coating. The SEM images of C3 are depicted in Fig. 4(e) and (f).

Most of the B- and N-rich areas were located in pores according to optical and scanning electron microscopy. The microstructural images of the coatings shown in Fig. 4 indicate that an unsuitable boron nitride distribution caused the higher porosities of the C2 and C3 coatings. High-magnification images of the B- and N-rich areas of these coatings are shown in Fig. 5. Boron nitride powder was melted using a plasma torch to create a new type of microstructure, as shown in Fig. 5(a) and (b) for the C2 and C3 coatings, respectively. Fig. 6 depicts the porosity of each coating. Similar to the metallographic results depicted in Fig. 4, the porosity of the C2 coating was higher than that of the C3 coating.

According to the coating porosities indicated in Fig. 6, the porosities of the C2 and C3 coatings increased due to the addition of h-BN, regardless of whether the starting powders were prepared using the blended process or the MA process. Based on the microstructures of the feedstock powders, the powder particle size was smaller after the MA process. According to previous studies, powders with smaller particle sizes can produce lower-porosity coatings [18], and the porosity of the C2 coating was higher than

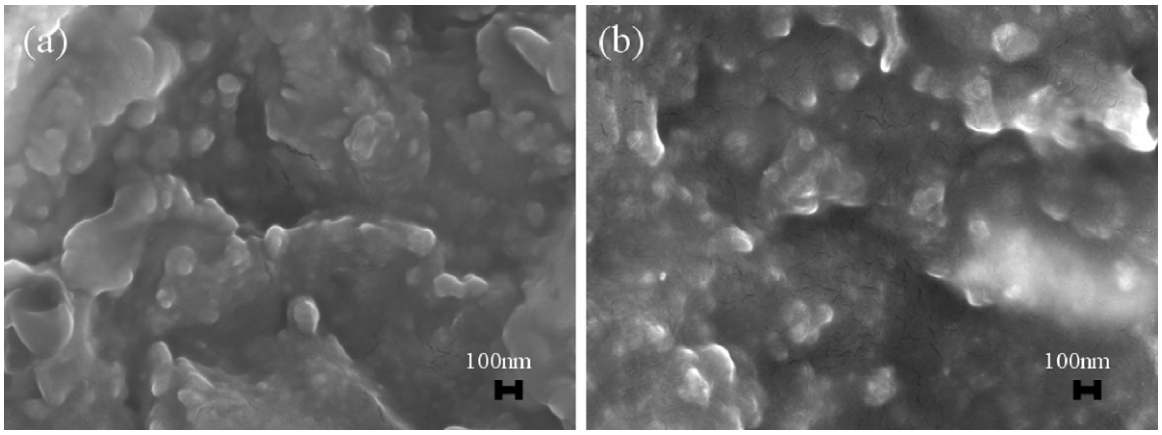

Fig. 5. High-magnification images of B- and N-rich areas of coatings: (a) C2 and (b) C3 coating.

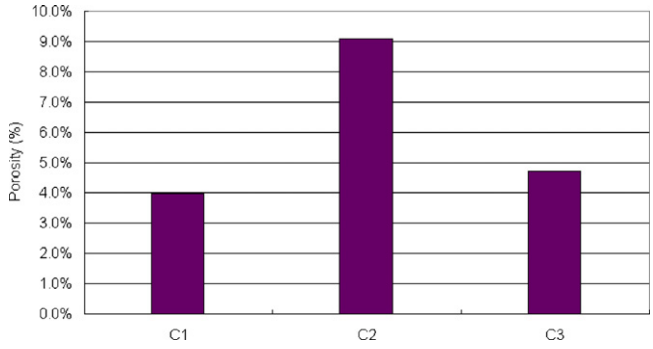

Fig. 6. The porosities of the coatings.

that of the C3 coating. However, more BN was incorporated into the C2 coating than the C3 coating (Fig. 4) due to the formation of BN near to the pores of these coatings. The porosities of the C2 and C3 coatings indicate that the blending process could potentially allow the Ni–Al particles to catch more BN compared to the MA process.

Fig. 7 depicts the XRD spectra of the powders and coatings at the h-BN (0 0 0 2) position. The C2 powder presents good crystallization. In the C3 powder, the peak intensity of h-BN (0 0 0 2) is reduced, which is similar to the finding that was reported by Tekmen et al. [19]. After the MA process, thick h-BN grains decomposed into many thinner layers that cleaved along the basal planes [20].

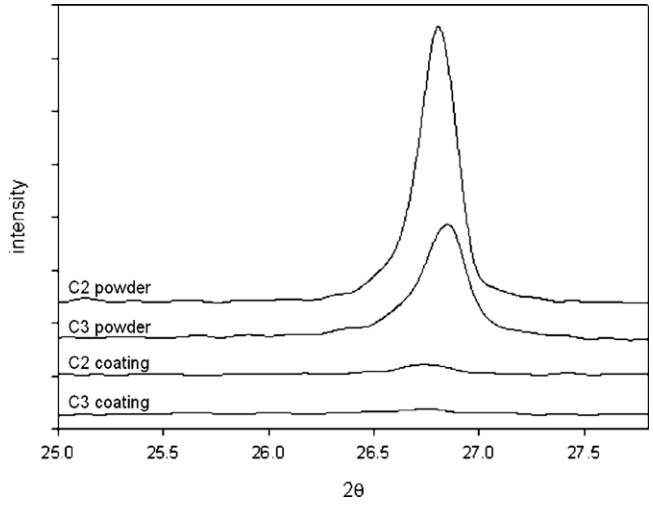

Fig. 7. X-ray diffraction spectra of the coatings along h-BN (0 0 0 2).

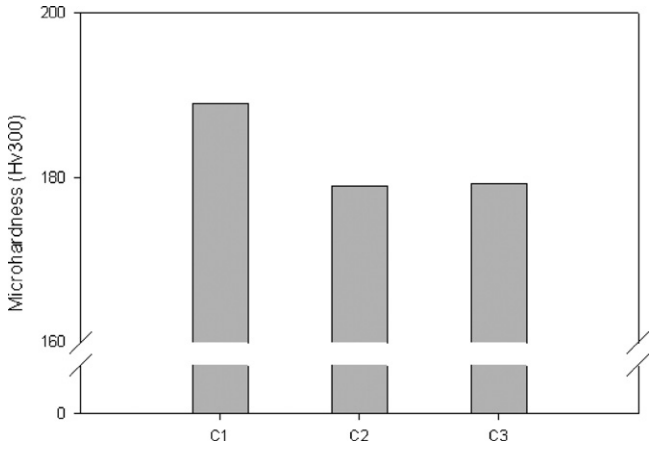

Fig. 8. Microhardnesses of the coatings.

Thus, the crystallization of the C3 powder was reduced after the MA process, as indicated by the XRD pattern. The c-BN or a-BN phases of h-BN were induced by the high pressure and temperature that was used during the thermal spraying process [21]. After plasma spraying, crystallization along h-BN (0 0 0 2) of the C2 coating was observed. The SEM images shown in Fig. 5 also demonstrate that the surface morphology of the BN was altered. Applied thermal and impact forces during plasma spraying caused the h-BN phase to transform into amorphous boron nitride (a-BN). The C3 coating

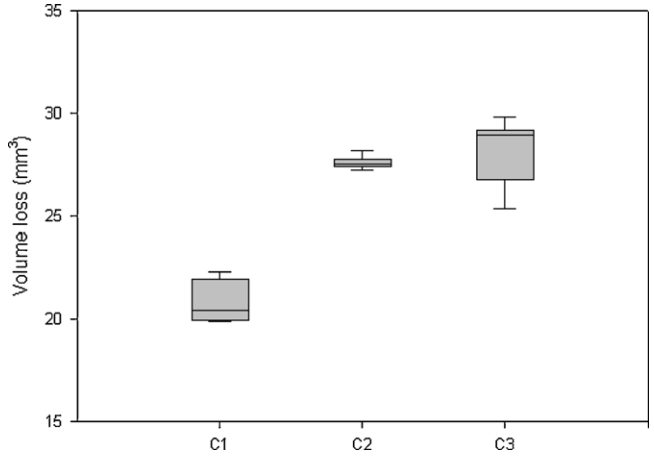

Fig. 9. Volume loss during dry sand wear testing.

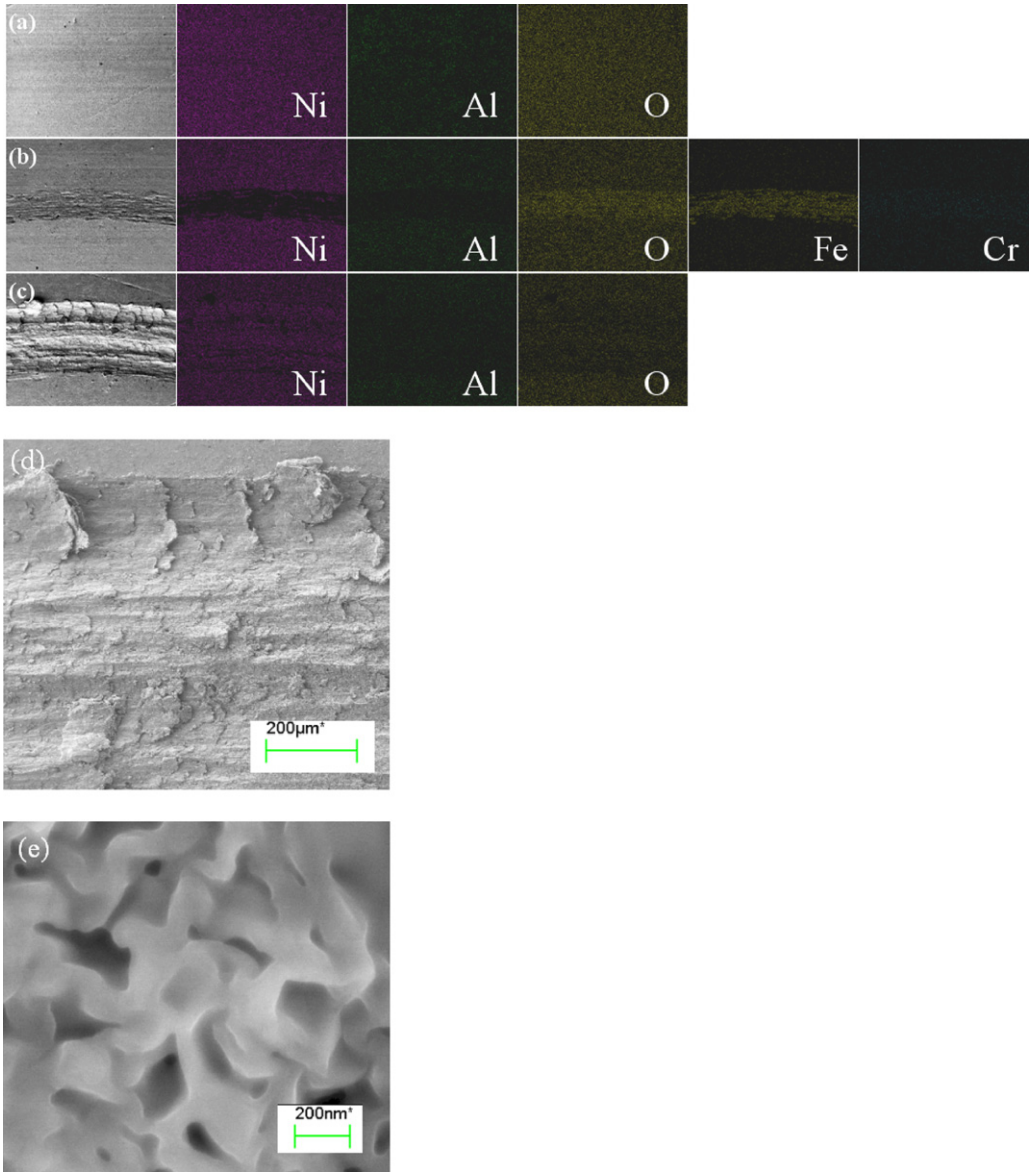

Fig. 10. SEM and EDS images of trace elements in coatings after ball-on-disk wear testing at 850 °C: (a) C1, (b) C2, (c) C3, (d) higher-magnification image of C3 coating, (e) higher-magnification image of C2 coating at Fe- and O-rich area.

also exhibited a lower degree crystallization along h-BN (0 0 0 2); however, the degree of crystallization of the C3 coating was lower than that of the C2 coating. Moreover, according to the XRD results, the peak intensity of the C3 coating was shifted to the left.

The microhardness of the Ni–Al coatings was reduced with the addition h-BN, as shown in Fig. 8. According to a previous article, the microhardness of a coating will normally decrease when a soft material is added [15]. In this case, the microhardnesses of the C2 and C3 coatings were lower than that of the C1 coating. After dry sand wear testing, the volume losses of the coatings increased when BN was added to the coating, as shown in Fig. 9. Because BN is softer than Ni–Al, the C2 and C3 coatings experienced greater volume losses than the C1 coating.

The C1 coating is a well-bonded thermally sprayed coating that exhibits a high bonding strength between its layers. The average bonding strength of the C1, C2 and C3 coatings were 9105, 7474 and 7328 psi, respectively. After adding h-BN to the coatings, the bonding strengths of the coatings were reduced. After ball-on-disk wear testing at 850 °C, elemental distribution images of the coating surfaces were obtained, as shown in Fig. 10(a–c). The wear trace was not significant in the C1 coating; however, the C2 coating elemental distribution image indicates the transfer of Fe from the surface of the steel-testing ball to the C2 coating surface. Additionally, partial peeling of the C3 coating was observed, as shown in Fig. 10(d). The weights lost by the C1, C2 and C3 coatings due to wear were 0.0003, −0.0018 and 0.0108 g, respectively. Based on the inspection of the SEM images of the powders that were presented earlier in this paper, the size of the Ni–Al particles in the C3 powder was refined after the MA process. Moreover, the BN material was distributed around the surface of the Ni–Al particles. After plasma spraying, the C3 coating that was created using a refined powder exhibited a greater Ni–Al/BN interfacial area in the coating. The greater Ni–Al/BN interfacial area between splat layers caused greater displacement due to the fact that BN is a soft material. The displacement of the splat layers caused weak bonding in the coating and thus, partial peeling under the high pressure of ball-on-disk wear testing. The partial peeling of the coating also caused the coefficient of friction to increase. The coefficients of friction of the C1, C2 and C3 coatings were 0.71, 0.70 and 2.31, respectively. The C2 coating exhibited better wear resistance than the other two coatings

(C1 and C3). High-magnification SEM images of the Fe- and O-rich areas that are shown in Fig. 10(e) indicate that the crystalline structures of iron oxides were induced. According to the EDS analysis in Fig. 10(a–c) and XRD analysis, no Fe was present in the plasma-sprayed coatings. The Fe must originate from the steel balls that were used during ball-on-disk testing. More BN was present in the C2 coating than in the C3 coating, as previously described in this article. A greater amount of the h-BN phase was transformed into the a-BN phase, as indicated in Fig. 7. The formation of a-BN phase that was induced in the C2 coating caused trace amounts of Fe to be transferred from the ball surfaces to the wear track of the C2 coating surface during ball-on-disk testing. The results indicate that the Fe- and O-rich areas on the wear tracks of the coatings were crystalline in structure. This suggests that the wear properties of Ni–Al coatings can be improved with the addition of BN by blending.

4. Conclusions

This study has investigated the structural evolution of nickel–aluminum (Ni–Al) alloys following the addition of hexagonal boron nitride and deposition using atmospheric plasma spraying. The major results of this study are summarized as follows:

1. Ni–Al/h-BN powders can be mixed and co-deposited as plasma-sprayed coatings.
2. The h-BN material displays lower degrees of crystallization along (0 0 0 2) after the MA process or plasma spraying. The thermal and impact forces that are introduced during plasma spraying can cause the h-BN phase to transform into amorphous boron nitride.
3. h-BN was found to exhibit a lubrication effect and provide a better tribological property when it was added to Ni–Al by blending.
4. When h-BN was decomposed into small particles which were imbedded in the splat boundaries, it would cause the splat structure to peel off and results in a poor wear property.

Appendix A. Supplementary data

Supplementary data associated with this article can be found, in the online version, at doi:10.1016/j.jallcom.2011.05.095.

References

[1] S. Kamal, R. Jayaganthan, S. Prakash, S. Kumar, J. Alloys Compd. 463 (2008) 358–372.
[2] S. Kamal, R. Jayaganthan, S. Prakash, J. Alloys Compd. 472 (2009) 378–389.
[3] S.B. Mishra, S. Prakash, K. Chandra, Wear 260 (2006) 422–432.
[4] A. Picas, A. Forn, G. Matthaus, Wear 261 (2006) 477–484.
[5] G. Bolelli, L. Lusvarghi, R. Giovanardi, Surf. Coat. Technol. 202 (2008) 4793–4809.
[6] E. Fleury, Y.-C. Kim, J.-S. Kim, D.-H. Kim, W.T. Kim, H.-S. Ahn, S.-M. Lee, J. Alloys Compd. 342 (2002) 321–325.
[7] N.L. Parthasarathi, M. Duraiselvam, J. Alloys Compd. 505 (2010) 824–831.
[8] R.A. Mahesh, R. Jayaganthan, S. Prakash, Mater. Sci. Eng. A 475 (2008) 327–335.
[9] R.A. Mahesh, R. Jayaganthan, S. Prakash, J. Alloys Compd. 460 (2008) 220–231.
[10] T. Saito, Y. Imada, F. Honda, Wear 236 (1999) 153–158.
[11] Y. Kimura, T. Wakabayashi, K. Okada, T. Wada, H. Nishikawa, Wear 232 (1999) 199–206.
[12] H.I. Faraoun, T. Grosdidier, J.-L. Seichepine, D. Goran, H. Aourag, C. Coddet, J. Zwick, N. Hopkins, Surf. Coat. Technol. 201 (2006) 2303–2312.
[13] M. Cherigui, N.E. Fenineche, G. Ji, T. Grosdidier, C. Coddet, J. Alloys Compd. 427 (2007) 281–290.
[14] M.H. Enayati, F. Karimzadeh, M. Tavoosi, B. Movahedi, A. Tahvilian, J. Therm. Spray Technol. 20 (2011) 440–446.
[15] Y. Tsunekawa, I. Ozdemir, M. Okumiya, J. Therm. Spray Technol. 15 (2006) 239–245.
[16] H.S. Ni, X.H. Liu, X.C. Chang, W.L. Hou, W. Liu, J.Q. Wang, J. Alloys Compd. 467 (2009) 163–167.
[17] M.M. Verdian, K. Raeissi, M. Salehi, J. Alloys Compd. 507 (2010) 42–46.
[18] X.Q. Liu, Y.G. Zheng, X.C. Chang, W.L. Hou, J.Q. Wang, Z. Tang, A. Burgess, J. Alloys Compd. 484 (2009) 300–307.
[19] C. Tekmen, I. Ozdemir, G. Fritsche, Y. Tsunekawa, Surf. Coat. Technol. 203 (2009) 2046–2051.
[20] J.Y. Huang, H. Yasuda, H. Mori, J. Am. Ceram. Soc. 83 (2000) 403–409.
[21] R. Goswami, H. Herrnan, S. Sampath, J. Parise, Y. Zhu, D. Welch, J. Am. Ceram. Soc. 85 (2002) 2437–2443.